Scientific Research Publishing

New Journal of Glass and Ceramics, 2022, 12, 1-18
https://www.scirp.org/journal/njgc
ISSN Online: 2161-7562
ISSN Print: 2161-7554

Studies of Anomalies in Mixed Conduction of Na_2O and V_2O_5 Doped Boro-Phosphate Glasses

Sangamesh Jakhati[1], Nagaraja Nadavalumane[1], JalandharRao Sonkamble Ashwajeet[2]

[1]Department of Physics, VTU-Research Centre, Rao Bahadur Y Mahabaleswarappa Engineering College, Ballari, India
[2]Department of Physics, Davangere University, Davanagere, India
Email: jakhati@gmail.com, nagphysics@gmail.com

How to cite this paper: Jakhati, S., Nadavalumane, N. and Ashwajeet, J.S. (2022) Studies of Anomalies in Mixed Conduction of Na_2O and V_2O_5 Doped Boro-Phosphate Glasses. *New Journal of Glass and Ceramics*, **12**, 1-18.
https://doi.org/10.4236/njgc.2022.121001

Received: September 29, 2022
Accepted: October 28, 2022
Published: October 31, 2022

Abstract

A set of borophosphate glasses doped with alkali and transition metal (TM) ions have been synthesized. The glasses were carried through; annealing, XRD, density, DC conductivity studies. Molar volume and density varied nonlinearly. High temperature activation energy is analysed taking into consideration of Mott's SPH model. The low temperature electrical conductivity was analysed by Mott and Greaves VRH. Several polaron hopping related parameters at high temperature region and density of states at low temperature region were computed. The high temperature DC activation energy measured by conductivity, calculated numerous pertained parameters varied nonlinearly with mole fraction of vanadium content. The Study exhibits DC electrical conduction is due to both alkali and transition metal ions and thus confirms the mixed conductivity. A crossover conduction mechanism from the ionic dominant region to polaronic predominant region has been also observed. Studies revealed the ***single transition effect*** at 0.4 mol fraction of V_2O_5 content.

Keywords

Borophosphate Glasses, Sodium, Vanadium, Single Alkali Effect (SAE), Single Transition Effect (STE)

1. Introduction

Research on solitary borate, phosphate and vanadate glasses are restricted owing to their hygroscopic nature. Nevertheless, interestingly phosphate glasses have exhibited enhanced chemical durability in combination with boron network [1]. In general, the alkali and TM ion doped borophosphate glasses encompass substantially many technological applications such as solid-state fuels in Batteries,

electrodes in solid state batteries, electrochemical applications, laser shielding materials and photonic biomedical fields [2] [3] [4] [5]. Phosphate glasses have some benefits over the silicate and borate glasses because of their glass forming ability [6]. From spectroscopic absorption bands and also due to hydroxyl groups has been verified the hygroscopic nature of phosphate glasses [7] [8] [9] [10]. With alkali oxides of Na cations, the phosphate glasses have improved their thermal stability [11]. These are very promising materials for physical, chemical, optical and medical applications because of their high stability, controlled aqueous solubility and transparency in the wide spectral region [12]. In $65P_2O_5$-$15BaO$-$5Al_2O_3$-$5ZnO$-$10Na_2O$ glass network added by B_2O_3 content, the hardness and flexural strength were found high up to 6 mol% boron content, which indicates the improvement in mechanical properties of glass by inclusion of boron [13]. The inclusion of alkali and TM ions in borophosphate glasses, increases the conductivity of the glass systems [14] [15] [16] [17]. The electrical conductivity in the single TM ion doped oxide glasses such as CuO, Fe_2O_3 and V_2O_5 is attributed to charge carrier hopping between lower and higher valency state of TM ion, for example, Cu^+ to Cu^{2+}, Co^{2+} to Co^{3+}, V^{4+} to V^{5+}, and so on, and nobody were reported the "*single transition effect*" [18] [19] [20]. The conductivity in single alkali doped oxide glasses is taking place by ion diffusion by hopping from one ionic site to another in the glass matrix [14] [21] [22] [23]. The electrical conductivity appears to be predominant in relevant to increased concentration in NiO and ZnO doped borophosphate glasses [24]. Few physicists reported the single alkali effect in many oxide glass systems and the conductivity was found to be mixed and the dominant conduction regimes were observed [25] [26]. In case of more than one alkali ion doped oxide glasses' ability to conduct was due to migration of alkali ions by hopping between two dissimilar ion sites in the glass matrix, and many of the glass systems were exhibited MAE [14] [18]-[23] [27] [28]. The primary purpose of this study is to conduct, a detailed understanding of the effect of doping borophosphate glasses with alkali and transition metal ions, from a systematic study on XRD, density at room temperature D and DC electrical properties across a wide range of temperature in $(B_2O_3)_{0.1} + (P_2O_5)_{0.4} + (Na_2O)_{0.5-x} + (V_2O_5)_x$, coded as BPVN, where x is 0.05, 0.1, 0.15, 0.2, 0.25, 0.3, 0.4, 0.45 BPVN glasses.

The study mainly reports to understand the variation of electrical conductivity as a result of migration of alkali ions, hopping of polarons, mixed conduction, dominant conduction mechanism, the anomaly effect such as single transition effect and the results were presented.

2. Experimental

2.1. Glass Preparation

The AR grade chemicals with 99% purity such as boric acid (H_3BO_3) from HI media, Ammonium dihydrogen ortho-phosphate ($NH_4H_2PO_4$) from Sd fine, Vanadium pentoxide (V_2O_5) from Sigma-Aldrich and Sodium carbonate (Na_2CO_3)

from Merc various international chemical making firms were selected and procured on swift accessibility basis. The chemicals were mixed for every calculated weight proportion of each glass system and transferred into an agate mortar and manually grinded to obtained molecular dimensions powder. The crushed mixture was shifted into infusil make scientific company made silica crucibles. The crucible was employed into high temperature electrical furnace and heated to a very high temperature of the order of 1223 K and left over for 2 hours. The melted mixture of liquid was quenched by putting it on a fine- grooved stainless-steel plate in the right shape and then quickly closing another plate on top of it. The glass fragments in the shape of a disc were gathered. By transferring the glasses into a muffle furnace, they were annealed at 523 K for about six hours to eliminate thermal strains if they exist in the glass matrix. After annealing, the samples were reshaped into fine dimensions using sandpaper and pile. The thickness of the glasses was calculated using digital screw gauge with precision of 0.01 mm and cross-sectional area using graph sheet with accuracy of 1 mm.

2.2. XRD

On each of the produced glasses, X-ray diffraction analyses were carried, using Malvern Panalytical X-ray diffractometer X'PERT^3 powder instrument operated at 40 kV and current of 30 mA with Cu-Kα wavelength at room temperature and 2θ ranging from 10˚ to 80˚.

2.3. Density

The glasses were subjected room temperature (RT) density studies by taking toluene as an immersion liquid with a density of 0.8669 g/cc and applying the Archimedes principle, by using citizen make A digital, single-pan balance with a precision of 0.1 mg. The RT density of the glasses were calculated by using succeeding Equation (1).

$$D = \left(\frac{M_a}{M_a - M_L} \right) D_L \tag{1}$$

Here, M_a stands for the weight of the glass samples when they are suspended in air; M_L refers to the weight of the sample when it is suspended in immersion liquid; and, D_L represents the density of immersion liquid, like toluene. The molar volume V_M was estimated from determined densities of the glasses using equation.

$$V = \frac{xM}{D} \tag{2}$$

Here x is molar fraction, M is the molecular weight and D is density of the glasses [29] [30].

2.4. DC Conductivity

The dc conductivity measurement was performed by painting conductive silver

paste on either side of the large surfaces and placing them in a two probe Keithley made instrument and applying constant voltage across the glasses over a wide temperature, from 303 K to 498 K. The current flowing through glass and voltage applied across the glass system was enumerated by using digital Pico ammeter and digital multi-meter with accuracy of ±10 mV. The Chromel-alumel thermocouples, with a precision of 1K, were used to measure the temperatures of the samples. The error on conductivity was determined using the relations and was in the range of 3% - 5% [14].

3. Results and Discussion

3.1. X-Ray Diffraction Studies

The x-ray diffraction pattern depicted in the subsequent **Figure 1** showed the non-existence of sharp peaks and confiding to the fact that the glasses lack crystalline structure. A bulge like structure can be noticed in the range between 18˚ to 38˚ revealing the existence of short-range atomic order [31].

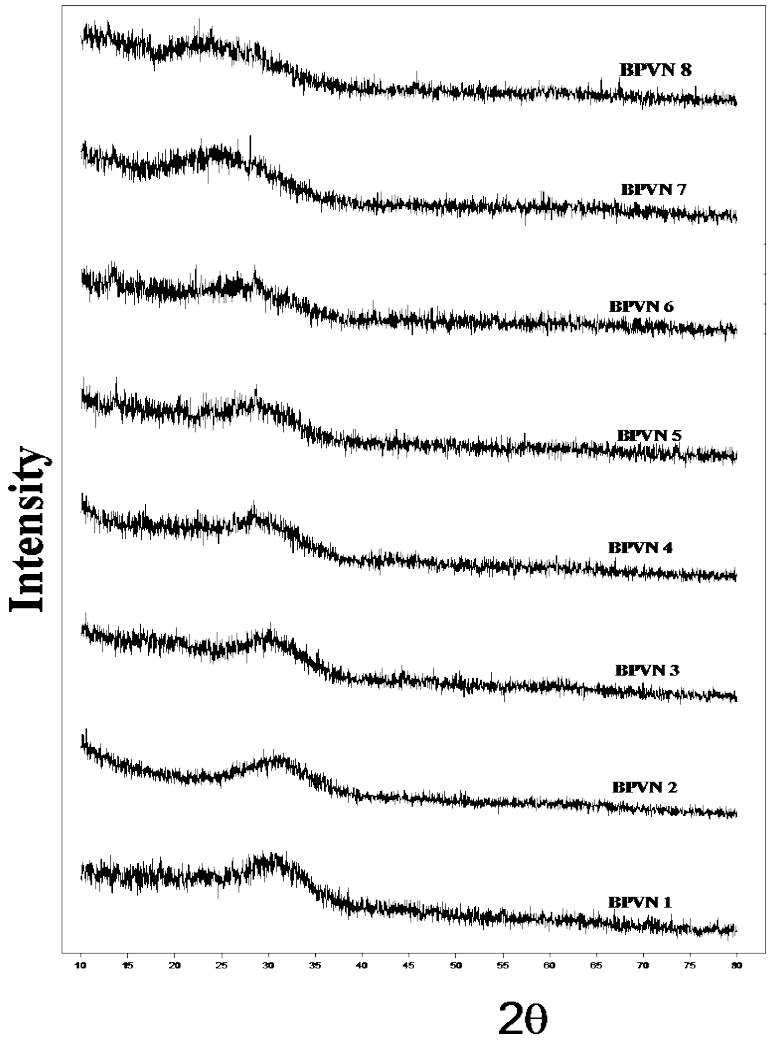

Figure 1. X-ray diffraction pattern of BPVN glasses.

3.2. Room Temperature Density Studies

The density and molar volume at room temperature of present glasses versus mole fractions of V_2O_5 are depicted in Figure 2. The measured density at room temperature and calculated molar volume of glasses were observed to be in the range of 0.943 g/cm^3 - 1.776 g/cm^3 and 8.130 cm^3/mol - 14.322 cm^3/mol respectively as recorded in the Table 1. With increasing V_2O_5 content up to 0.15 mole fractions, the density of the current glasses dropped and hits minimum value and thereafter, it has been observed density rose nonlinearly with increasing V_2O_5 concentration up to a mole fraction of 0.4 before decreasing again at 0.45 mole fraction of V_2O_5 content. The glasses' molar volume was varied appositively as density. Figure 2 shows how density and molar volume change with increasing V_2O_5 content. Density and molar volume estimates agreed well with various alkali and TM-doped glasses [14] [32] [33].

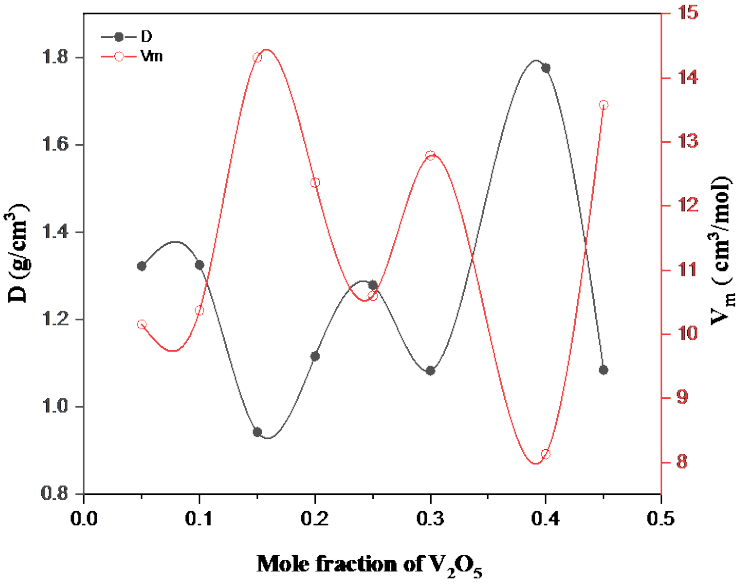

Figure 2. Variation in D and V_M as a function of mole fractions of V_2O_5.

Table 1. Physical properties of BPVN glasses.

Glass	Mole fraction, X	D (g/cm^3)	V_M (cm^3/mol)	$N\times 10^{21}$ (eV^{-1}/m^3)	R (nm)	r_p (nm)
BPVN1	0.05	1.323	10.155	0.438	1.317	0.531
BPVN2	0.1	1.325	10.372	0.878	1.044	0.421
BPVN3	0.15	0.943	14.322	0.936	1.022	0.412
BPVN4	0.2	1.116	12.365	1.479	0.878	0.354
BPVN5	0.25	1.280	10.602	2.118	0.779	0.314
BPVN6	0.3	1.083	12.791	2.152	0.775	0.312
BPVN7	0.4	1.776	8.130	4.705	0.597	0.241
BPVN8	0.45	1.085	13.579	3.233	0.676	0.273

The mean transition metal ion distance was calculated using, $R = \left(\frac{1}{N}\right)^{1/3}$ here, N represents the concentration of total TM ion that was calculated using the relationship $N = 2(Dx/M) \times N_A$, here D is the density, x is the mole fraction of TM ion and M is the molecular wt. of the respective ions of the corresponding glass system, N_A is Avogadro number.

The density of the present glasses decreased and molar volume increased with increase in the V_2O_5 content up to $x = 0.15$ mol fraction of vanadium oxide concentration (TM ions). This demonstrates that the glass network structure was relaxed and a rise in the number of vanadium ions Up to $x = 0.25$ mole fractions of vanadium ion content, the density of glasses increased while molar volume declined, which reveals that in this region, the topology of the glasses was jittery. Further increase of V_2O_5 concentration the density decreased and molar volume increased until $x = 0.4$ mol fraction of vanadium ion and hits peak value. And again, increase of vanadium ion concentration the density decreased up to $x = 0.45$ mole fractions of V_2O_5 content. The molar volume behaves oppositely as density. Hence the topology of the present glasses was continuously varied nonlinearly with increase of V_2O_5 content which was incorporated into a glass structure. The glass network structure opened and jittered nonlinearly with mole fractions of V_2O_5 ranging from $x = 0.05$ to 0.45 at the expense of sodium ion concentration. In the current set of glasses, the alkali ion Na_2O concentration was replaced by Transition metal ion V_2O_5 from $x = 0.05$ to 0.45, from the analysis of density and molar volume indicating that the topology of glass network continuously alters nonlinearly and It indicates the presence of a single transition ion effect at $x = 0.4$ mole fraction of V_2O_5 content. This is the first-time boro phosphate glasses doped with Na_2O and V_2O_5 explored to density and molar volume studies and exhibited transition effect which was not observed in any earlier reports [14].

3.3. DC Conductivity

The thickness and cross-sectional area that have been measured, ranging from 2.01 mm to 2.90 mm and from 16 mm^2 to 51 mm^2 respectively. The present glasses dc conductivity was estimated at 573 K and lies between 4.48×10^{-5} $(\Omega \cdot m)^{-1}$ to 7.94×10^{-3} $(\Omega \cdot m)^{-1}$ and hence which are semiconducting in nature [20] [32] [34].

In **Figure 3**, we see a graph of $\ln(T)$ vs $(1/T)$ that was generated using Mott's Small polaron hopping (SPH) model for current existing glasses [19] [35] [36] [37].

In the non-adiabatic conduction region, the linear lines were fits to the graph, above $T = \frac{\theta_D}{2}$ subsequently the corresponding activation energy W for all glasses were estimated and were in the range of 0.232 eV to 0.696 eV. These values are comparable to many published values of Alkali and TM ion glass systems

[25] [32] [38] [39]. For present series of glasses, the dc electrical conductivity at 468 K, as well as the calculated high temperature activation energies, were plotted and illustrated in Figure 4.

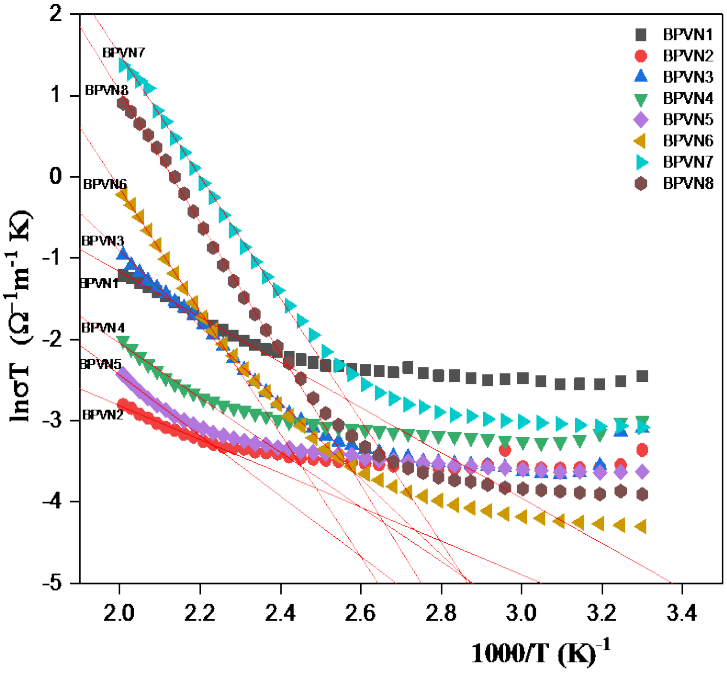

Figure 3. Plots of $\ln\sigma T$ vs $1/T$ for BPVN glasses. Solid lines are LS fits to the data.

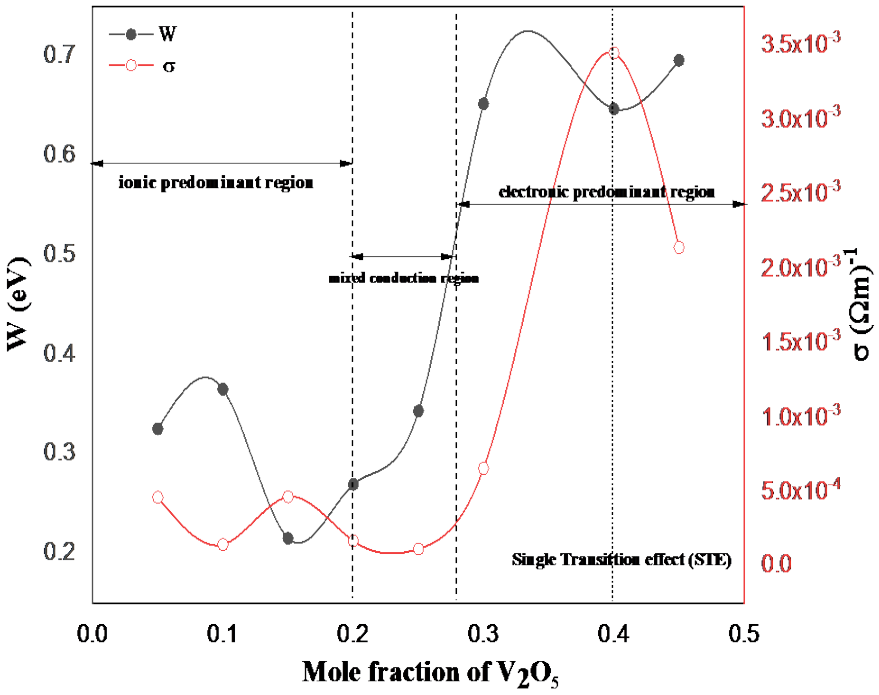

Figure 4. High temperature activation energy (W) and conductivity (σ) plotted as a function of mole fraction at 468 K.

It is observed, at $x = 0.15$ mole fractions of V_2O_5, the high temperature activation energy reduces and the dc electrical conductivity rises, as seen in Figure 4, and further growth of V_2O_5 content, As the activation energy W rises, the conductivity σ falls, and further growth of vanadium content in the glass structure the conductivity increases and activation energy decreases until 0.4 mol fraction of V_2O_5 and further increase of vanadium the conductivity diminishes and activation energy raises further again. The incorporation of V_2O_5 content, high temperature DC activation energy and the DC conductivity varies oppositely and conductivity increases and hit peak value at 0.4 mol V_2O_5 and conductivity decrease from 0.4 mol to 0.45 mol of V_2O_5 the same values were tabulated in Table 2. It is clear in Figure 4 that from 0.05 to 0.2 mol of V_2O_5 content glasses reveals the ionic predominant region and from 0.2 to 0.3 mol fraction of V_2O_5 content shows mixed conduction region and form from 0.3 onwards up to 0.45 mol of V_2O_5 content reveals the electronic predominant region. Hence in the current series of BPVN glasses the varying conductivity and activation energy with V_2O_5 mole fraction exhibit the 'single Transition Effect' (STE) at $x = 0.4$ mole fraction of vanadium content in glass matrix. Because of the addition of V_2O_5 content at the cost of Na concentration, both sodium ions and polarons contribute to conductivity. Hence, the observed increase in conductivity at 0.15 mole fraction of V_2O_5 from 0.05 content demonstrates that alkali ions are responsible for the conductivity, indicating ionic predominant region and from 0.2 to around 0.25 mole fraction of V_2O_5 content shows mixed conductivity both due to alkali ions and transition metal ions. Further, from 0.3 to up to 0.45 mole fraction of V_2O_5 content is electronic predominant region and the conductivity is due to only polarons. Similar electronic predominant variations were found in several literatures [25] [40] [41] [42], which have been depicted in Figure 4

Conductivity in the non-adiabatic regime is governed by the Mott's SPH model and is given by

$$\sigma T = \sigma_o e^{-\frac{W}{k_B T}} \tag{3}$$

Table 2. Various polaron hopping related parameters of BPVN glasses.

Glass	Mole fraction of V_2O_5	W	σ at 468 K	ε_p	W_H	W_P	W_D
	X	(eV)	$(\Omega\cdot m)^{-1}$		(eV)	(eV)	(eV)
BPVN1	0.05	0.325	4.574×10^{-4}	21.633	10.155	0.388	0.262
BPVN2	0.1	0.365	1.409×10^{-4}	46.321	10.372	0.436	0.294
BPVN3	0.15	0.215	4.614×10^{-4}	33.787	14.322	0.257	0.173
BPVN4	0.2	0.269	1.667×10^{-4}	37.279	12.365	0.321	0.217
BPVN5	0.25	0.343	1.118×10^{-4}	44.628	10.602	0.410	0.276
BPVN6	0.3	0.652	6.520×10^{-4}	24.814	12.791	0.778	0.526
BPVN7	0.4	0.647	3.439×10^{-3}	34.010	8.130	0.772	0.522
BPVN8	0.45	0.696	2.134×10^{-3}	23.846	13.579	0.831	0.561

Here, W is the activation energy and σ_o is the pre-exponential term, and it is denoted as

$$\sigma_o = \upsilon_o N e^2 R^2 C(1-C) \mathrm{e}^{-\frac{2\alpha R}{k_B}} \tag{4}$$

Here, $\upsilon_o = \theta_D k_B / h$ is the optical phonon frequency, θ_D is the Debye temperature, N, R have their regular meanings, as previously stated. α is the tunnelling factor and C is reduced fraction TM ions concentration [25].

It is taken into account for the strong electron-phonon interaction proposed by Austin and Mott [37],

$$W \begin{cases} = W_H + W_D/2T & > \theta_D/2 \\ \cong W_D T & < \theta_D/4 \end{cases} \tag{5}$$

Here, $W_H = W_P/2$ is polaron hopping energy, W_D e is disorder energy occurring due to a disparity in the energy levels of nearby neighbours between two hopping sites. The polaron energy W_H is estimated by Greaves model [33] given as

$$W_H = \frac{W_P}{2} = \frac{e^2}{4\varepsilon_p}\left(\frac{1}{r_p} - \frac{1}{R}\right) \tag{6}$$

Here W_P is the polaron binding energy and ε_p is the effective dielectric constant and is given by

$$\varepsilon_p = \frac{e^2}{4Wr_p} \tag{7}$$

Here r_p is small polaron radius and given as

$$r_p = \frac{1}{2}\left(\frac{\pi}{6N}\right)^{1/3} \tag{8}$$

The calculated data for ε_p and r_p are tabulated in the **Table 2** and they are similar to the reported data in the literature [25] [33] [39] [42] [43].

The polaron bandwidth J^{SPH} according SPH model [37] [44] is given by

$$J^{SPH} \begin{cases} > (2KTW_H/\pi)^{\frac{1}{4}} (h\nu_o/\pi)^{\frac{1}{2}} & \text{for adiabatic SPH} \\ < (2KTW_H/\pi)^{\frac{1}{4}} (h\nu_o/\pi)^{\frac{1}{2}} & \text{for non-adiabatic SPH} \end{cases}$$

Using the relation $J_{th} = J_o \mathrm{e}^{-2\alpha R}$, were determined to fall within the acceptable range of 0.017 eV to 0.020 eV and, here $J_o = \frac{(W_H)_{\min}}{4}$ [18] varies from 0.032 eV to 0.104 eV and same recorded in **Table 3** in that same table it's found that the values of J_{wh} fulfils both the Holstein condition for the creation of small polaron hopping and the non-adiabatic SPH conduction, which is given in the equation above. These conditions are necessary for the formation of small polaron hopping [45], that were observed in the limit of 0.043 eV to 0.138 eV represented in the **Table 3**, the value of $\alpha = 20(\mathrm{nm})^{-1}$ in earlier equation is according to reports various TM ion doped glasses [44]. The relationship [45]

was used to calculate the density of states at the fermi level $N(E_F)$, $N(E_F) = 3/4\pi R^3 W$, and vary as to the order of 10^{26} $eV^{-1}m^{-3}$ - 10^{27} $eV^{-1}m^{-3}$ and shown in **Table 3** and the reported values agree with various such glasses systems [14] [32] [46]. The small polaron hopping constant γ_P, is essential in understanding electron-phonon interaction, hence estimated by the relation $\gamma_P = 2W_H/h\nu_o$ and is presented in **Table 3**. In accordance with Austin & Mott [37], when $\gamma_P > 4$ suggests an interaction between electrons and phonons in glasses.

3.4. Variable Range Hopping (VRH) Conductivity

At temperatures lesser than the Debye temperature, the DC conductivity were observed to exhibiting temperature dependent nonlinear variations, and signifying the prominent role of disorder energy due to which hopping of electron may happen between the nearest neighbors [35] [45] is given by

$$\sigma = A\mathrm{e}^{B/T^{-1/4}} \tag{9}$$

Here, $A = 4\left[2\alpha^3/9\pi kN(E_F)\right]^{\frac{1}{4}}$

$$B = \left[e^2/2(8\pi)^{\frac{1}{2}}\right]\upsilon_0\left[N(E_F)/\alpha kT\right]^{\frac{1}{2}}$$

From slopes of graph $\ln\sigma$ Vs $T^{-1/4}$ plotted in the **Figure 5** the values of A, B are found.

The estimated values of $N(E_F)$ are in the range of 10^{31} $eV^{-1}m^{-3}$ to 10^{40} $eV^{-1}m^{-3}$ as recorded in **Table 4** and it is clear that values determined are very much higher and deviate from the values comprising oxide glasses.

In the same low temperature range, lesser than the Debye temperature, variable range hopping (VRH) has been analysed in the light of Greave's VRH model and is given by

$$\sigma T^{1/2} = A\mathrm{e}^{-B/T^{1/4}} \tag{10}$$

Table 3. Polaron bandwidth and other related physical properties of BPVN glasses.

Glass	Mole fraction of V_2O_5	J^{SPH}	J_o	J_{wh}	J_{th}	$\upsilon_o \times 10^{12}$	$N(E_F)$	γ_p
	X	(eV)	(eV)	(eV)	(eV)	Hz	($eV^{-1}·m^{-3}$)	
BPVN1	0.05	0.017	0.049	0.065	1.76937×10^{-13}	4.561	5.719×10^{26}	20.566
BPVN2	0.1	0.018	0.054	0.073	4.6164×10^{-11}	4.613	1.021×10^{27}	22.836
BPVN3	0.15	0.015	0.032	0.043	4.24528×10^{-11}	4.249	1.848×10^{27}	14.605
BPVN4	0.2	0.017	0.040	0.054	9.53412×10^{-10}	4.665	2.333×10^{27}	16.642
BPVN5	0.25	0.018	0.051	0.068	8.82861×10^{-09}	4.821	2.621×10^{27}	20.533
BPVN6	0.3	0.020	0.097	0.130	1.82248×10^{-08}	4.613	1.401×10^{27}	40.792
BPVN7	0.4	0.019	0.097	0.129	6.32661×10^{-07}	4.301	3.086×10^{27}	43.419
BPVN8	0.45	0.020	0.104	0.138	1.38822×10^{-07}	4.301	1.972×10^{27}	46.708

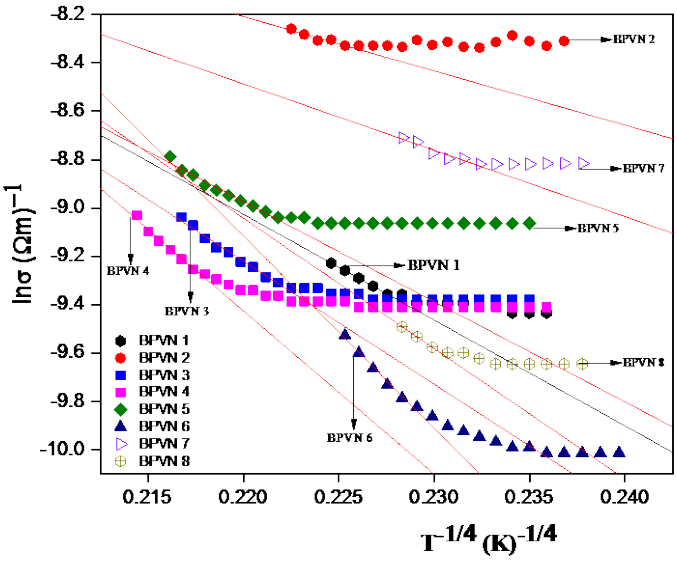

Figure 5. Plots of $\ln\sigma$ vs $T^{-1/4}$ for BPVN glasses. Solid lines are linear square fit to the data.

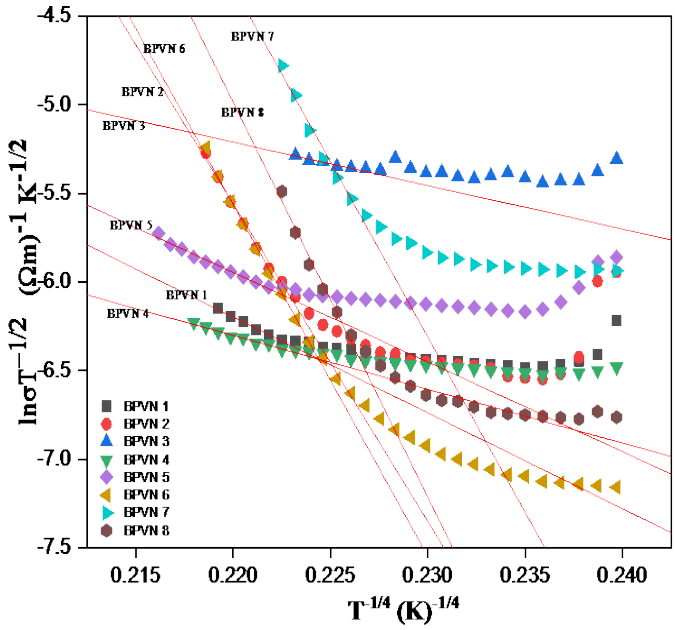

Figure 6. Plots of $\ln\sigma T^{-1/2}$ versus $T^{-1/4}$ for BPVN glasses. Solid lines areLS fits to the data.

Here A, B are constants and are determined from the least square (LS) fits to data in the plot of $\ln\sigma T^{-1/2}$ Vs $T^{-1/4}$ is shown in **Figure 6**

The density of states $N(E_F)$ was measured from the theoretical expression for constant B and given by

$$B = 2.1\left[\alpha^3/k_B N(E_F)\right]^{\frac{1}{4}}$$

The values of $N(E_F)$ varies from 10^{26} $eV^{-1}m^{-3}$ to 10^{30} $eV^{-1}m^{-3}$ and both are presented in **Table 4**, found to be in agreement with the several determined val-

ues by Greave's VRH model for alkali and TM ion doped oxide glasses [16] [25] [32] [40] [42] [47]. Thus, it may be concluded that the Greaves VRH model is sufficient to explain the electrical conductivity data in the temperature range lesser than the Debye temperature for the present glasses.

3.5. Charge Carrier Mobility and Density

According to N.F. Mott and E.A. Davis [36], N.F. Mott and I. Austin [37], in the adiabatic and non-adiabatic hopping regime carrier mobility μ, which involves electron diffusion via polaron hopping furnished in following

$$\mu = \left(\frac{\upsilon_o e R^2}{kT}\right) \mathrm{e}^{\frac{-W}{kT}} \quad \text{For adiabatic} \tag{11}$$

$$\mu = \left(\frac{eR^2}{kT}\right)\left(\frac{1}{\hbar}\right)\left(\frac{\pi}{4W_H kT}\right)^{\frac{1}{2}} J^2 \mathrm{e}^{\frac{-W}{kT}} \quad \text{For non-adiabatic} \tag{12}$$

carrier mobility μ were calculated at temperature of 195˚C and found to vary from 9.710×10^{-9} to 1.091×10^{-6} [18], the hopping carrier concentration N_C estimated from $\sigma = eN_C\mu$ [42], and it ranges from 5.719×10^{26} $eV^{-1}\cdot m^{-3}$ to 3.086×10^{27} $eV^{-1}\cdot m^{-3}$ and both are presented in **Table 5**.

The mobility and charge carrier density versus mole fractions of V_2O_5 content is shown in **Figure 7**. From the graph it is observed that up to 0.2 mole concentration of V_2O_5 the mobility decreases from starting 0.05 mol of V_2O_5 content, further increase in the V_2O_5 content the mobility is increases attains maximum value, then after, it keeps falling down continuously with growth of V_2O_5 content in the glass maximum until it reaches bare minimum value at $x = 0.45$ mole fraction, but At the same time, the largest concentration of charge carriers occurs at this location, suggesting Anderson's localization [48] [49] of charge carriers taking place around vanadium ions where glass network becomes more closed the presence of the Single Transition Effect (STE) at 0.4 mol fraction of V_2O_5 content in the glass matrix. It's very clear in similar **Figure 7** that, with increasing V_2O_5 content, charge carrier density acts practically opposite to mobility [50].

Table 4. Density of states, extracted from MVRH and GVRH of BPVN glasses.

Samples	$N(E_F)$ Moot's VRH	$N(E_F)$ Greave's VRH
	($eV^{-1}\cdot m^{-3}$)	($eV^{-1}\cdot m^{-3}$)
BPVN1	1.281×10^{38}	1.167×10^{29}
BPVN2	7.065×10^{31}	9.674×10^{26}
BPVN3	5.270×10^{34}	2.773×10^{30}
BPVN4	8.715×10^{34}	1.173×10^{30}
BPVN5	6.508×10^{40}	1.528×10^{29}
BPVN6	2.341×10^{31}	6.435×10^{26}
BPVN7	1.398×10^{31}	6.534×10^{26}
BPVN8	1.810×10^{31}	4.054×10^{26}

Table 5. Mobility and charge carrier concentrations of BPVN glasses.

Glass	Mole fraction of V_2O_5	μ	N_C
	X	m^2/Vs	$(eV^{-1}\cdot m^{-3}$
BPVN1	0.05	2.831×10^{-6}	5.719×10^{26}
BPVN2	0.1	1.091×10^{-6}	1.021×10^{27}
BPVN3	0.15	6.303×10^{-6}	1.848×10^{27}
BPVN4	0.2	2.595×10^{-6}	2.333×10^{27}
BPVN5	0.25	8.351×10^{-7}	2.621×10^{27}
BPVN6	0.3	1.648×10^{-8}	1.401×10^{27}
BPVN7	0.4	9.710×10^{-9}	3.086×10^{27}
BPVN8	0.45	6.749×10^{-9}	1.972×10^{27}

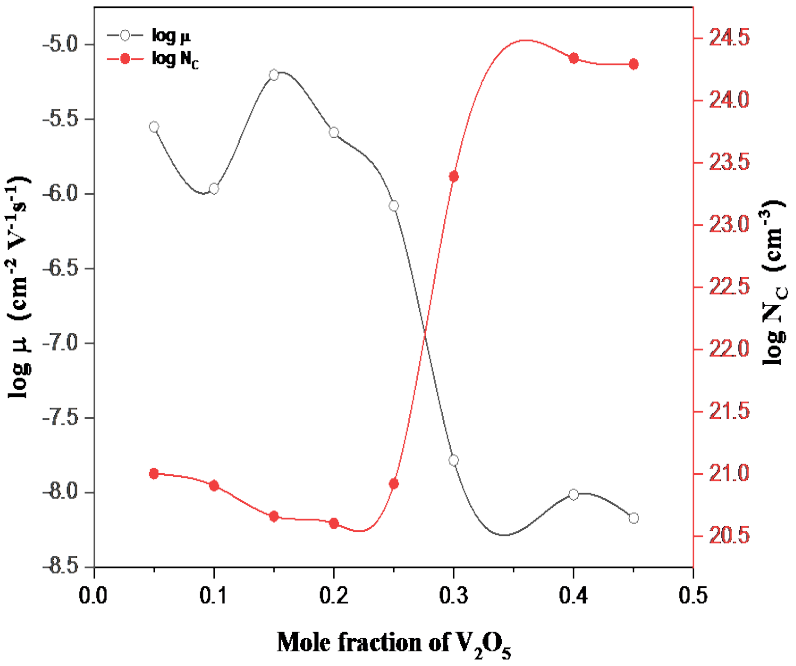

Figure 7. The mobility mat 468 K and charge carrier density, N_O versus mole fraction of V_2O_5.

4. Conclusions

The present study focused on investigation of room temperature density, DC electrical studies of alkali and TMI doped borophosphate glasses. The following observations have been found

1) XRD studies reveal that the present glasses were non-crystalline in nature.

2) From room temperature density molar volume was estimated, various parameters related to the density viz., R, r_p and $N(E_F)$ were estimated and Physical parameters vary nonlinearly with vanadium ion content at the cost sodium ion concentration.

3) DC electrical studies were carried out from room temperature to 473 K and

high temperature activation energy were calculated using Mott's SPH model, it is shown that the present glasses show the semiconducting nature.

4) The activation energy (W) and Conductivity at 468 K with mole fractions of V_2O_5 content, from 0.05 to 0.2 mol of V_2O_5 content glasses reveals the ionic predominant region and from 0.2 to 0.3 mol fraction of V_2O_5 content shows mixed conduction region and form from 0.3 onwards up to 0.5 mol of V_2O_5 content reveals the electronic predominant region which exhibits the single transition effect (STE) in the present glasses.

5) At temperatures lesser than the Debye temperature, conductivity was observed to exhibit temperature dependent nonlinear variations, and signifying the prominent role of disorder energy due to which hopping of electron may happen between the nearest neighbors which indicates the conduction process was due to single phonon aided motion.

6) Mott's and Mott and Greaves VRH models were used for low temperature region of conductivity data analysis and $N(E_F)$ values were estimated. The temperature independent conductivity was revealed that the conductivity due to multiphoton assisted motion. Which is indication of polaron hopping was beyond the nearest neighbors' ionic sites.

Conflicts of Interest

The authors declare no conflicts of interest regarding the publication of this paper.

References

[1] Karabulut, M., Yuce, B., Bozdogan, O., Ertap, H. and Mammadov, G.M. (2011) Effect of Boron Addition on the Structure and Properties of Iron Phosphate Glasses. *Journal of Non-Crystalline Solids*, **357**, 1455-1462. https://doi.org/10.1016/j.jnoncrysol.2010.11.023

[2] Famprikis, T., Canepa, P., Dawson, J.A., Islam, M.S. and Masquelier, C. (2019) Fundamentals of Inorganic Solid-State Electrolytes for Batteries. *Nature Materials*, **18**, 127-1291. https://doi.org/10.1038/s41563-019-0431-3

[3] Khan, S. and Singh, K. (2020) Structural, Optical, Thermal and Conducting Properties of $V_{2-x}Li_xO_5$-δ ($0.15 \leq x \leq 0.30$) Systems. *Scientific Reports*, **10**, Article No. 1089. https://doi.org/10.1038/s41598-020-57836-8

[4] Jha, A. (2016) Inorganic Glasses for Photonics: Fundamentals, Engineering, and Applications. Wiley, Hoboken. https://doi.org/10.1002/9781118696088 https://books.google.com/books?hl=en&lr=&id=R6DLCgAAQBAJ&oi=fnd&pg=PR13&dq=A.+Jha,+Inorganic+Glasses+for+Photonics:+Fundamentals,+Engineering,+and+Applications.+2016.+Accessed:+Jun.+06,+2022.&ots=mIPuE6BTQF&sig=PkEPw8QdfU17UWctktvqyPDpFn8

[5] Abouhaswa, A.S., Rammah, Y.S. and Turky, G.M. (2020) Characterization of Zinc Lead-Borate Glasses Doped with Fe^{3+} Ions: Optical, Dielectric, and Ac-Conductivity Investigations. *Journal of Materials Science: Materials in Electronics*, **31**, 17044-17054. https://doi.org/10.1007/s10854-020-04262-1

[6] Aliyu, A.M. and Ahmed, N.E. (2019) Structure and Physical Properties of $30MgSO_4$-(70-x) P_2O_5-xSm_2O_3 Glasses. *EDUCATUM Journal of Science, Mathematics and Technology*, **6**, 22-34. https://doi.org/10.37134/ejsmt.vol6.2.3.2019

[7] Łapa, A., Cresswell, M., Campbell, I., Jackson, P., Goldmann, W.H., Detsch, R. and

Boccaccini, A.R. (2020) Gallium- and Cerium-Doped Phosphate Glasses with Antibacterial Properties for Medical Applications. *Advanced Engineering Materials*, **22**, Article ID: 1901577. https://doi.org/10.1002/adem.201901577

[8] Sekhar, A.V., Pavić, L., Moguš-Milanković, A., Kumar, V.R., Reddy, A.S.S., Raju, G.N. and Veeraiah, N. (2020) Dielectric Dispersion and Impedance Spectroscopy of NiO Doped Li_2SO_4-MgO-P_2O_5 Glass System. *Journal of Alloys and Compounds*, **824**, Article ID: 153907. https://doi.org/10.1016/j.jallcom.2020.153907

[9] Huerta, E.F., Soriano-Romero, O., Meza-Rocha, A.N., Bordignon, S., Speghini, A. and Caldiño, U. (2020) Lithium-Aluminum-Zinc Phosphate Glasses Activated with Sm^{3+}, Sm^{3+}/Eu^{3+} and Sm^{3+}/Tb^{3+} for Reddish-Orange and White Light Generation. *Journal of Alloys and Compounds*, **846**, Article ID: 156332. https://doi.org/10.1016/j.jallcom.2020.156332

[10] Jupri, S.A., Ghoshal, S.K., Yusof, N.N., Omar, M.F., Hamzah, K. and Krishnan, G. (2020) Influence of Surface Plasmon Resonance of Ag Nanoparticles on Photoluminescence of Ho^{3+} Ions in Magnesium-Zinc-Sulfophosphate Glass System. *Optics & Laser Technology*, **126**, Article ID: 106134. https://doi.org/10.1016/j.optlastec.2020.106134

[11] Mondal, R., Biswas, D., Das, A.S., Ningthemcha, R.K.N., Deb, D., Bhattacharya, S., Kabi, S. (2020) Influence of Samarium Content on Structural, Thermal, Linear and Non-Linear Optical Properties of ZnO-TeO_2-P_2O_5 Glasses. *Materials Chemistry and Physics*, **255**, Article ID: 123561. https://doi.org/10.1016/j.matchemphys.2020.123561

[12] Ravangvong, S., Chanthima, N., Rajaramakrishna, R., Kim, H.J. and Kaewkhao, J. (2020) Effect of Sodium Oxide and Sodium Fluoride in Gadolinium Phosphate Glasses Doped with Eu_2O_3 Content. *Journal of Luminescence*, **219**, Article ID: 116950. https://doi.org/10.1016/j.jlumin.2019.116950

[13] Zhao, Y., Zhou, Y., Yang, J., Li, Y., Cheng, L., Wang, K., Sun, X., Sun, C. and Qin, Z. (2020) Optimized Structural and Mechanical Properties of Borophosphate Glass. *Ceramics International*, **46**, 9025-9029. https://doi.org/10.1016/j.ceramint.2019.12.150

[14] Nagaraja, N., Sankarappa, T. and Prashant Kumar, M. (2008) Electrical Conductivity Studies in Single and Mixed Alkali Doped Cobalt-Borate Glasses. *Journal of Non-Crystalline Solids*, **354**, 1503-1508. https://doi.org/10.1016/j.jnoncrysol.2007.08.042

[15] Song, J., Wu, D., Zhang, C., Ming, Q. and Imanzadeh, M. (2022) Investigation of Mixed Alkali Effect on the DC Electrical Conductivity, Structural, and Physical Properties of Phosphate Glasses Containing MnO_2. *Journal of Physics and Chemistry of Solids*, **167**, Article ID: 110759. https://doi.org/10.1016/j.jpcs.2022.110759

[16] El-Desoky, M.M., Wally, N.K., Sheha, E. and Kamal, B.M. (2021) Impact of Sodium Oxide, Sulfide, and Fluoride-Doped Vanadium Phosphate Glasses on the Thermoelectric Power and Electrical Properties: Structure Analysis and Conduction Mechanism. *Journal of Materials Science: Materials in Electronics*, **32**, 3699-3712. https://doi.org/10.1007/s10854-020-05115-7

[17] Ashwajeet, J.S., Sankarappa, T., Ramanna, R., Sujatha, T., Nagaraja, N. and Vijayakumar, B. (2015) Electrical Conduction in Borophosphate Glasses Doped With CoO and Li_2O. *Research Journal of Material Sciences*, **3**, 1-6. https://www.researchgate.net/profile/Dr-J-S/publication/290482639_Electrical_Conduction_in_Borophosphate_Glasses_Doped_with_CoO_and_Li2O/links/5d1ee735299bf1547c98b3cb/Electrical-Conduction-in-Borophosphate-Glasses-Doped-with-CoO-and-Li2O.pdf

[18] Sega, K., Kuroda, Y. and Sega, K. (1998) D.C. Conductivity of V_2O_5-MnO-TeO_2 Glasses. *Journal of Materials Science*, **33**, 1303-1308. https://doi.org/10.1023/A:1004302431797

[19] Mott, N.F. (1968) Conduction in Glasses Containing Transition Metal Ions. *Journal of Non-Crystalline Solids*, **1**, 1-17. https://doi.org/10.1016/0022-3093(68)90002-1

[20] Kumar, B.V., Sankarappa, T., Kumar, M.P. and Kumar, S. (2009) Electronic Transport Properties of Mixed Transition Metal Ions Doped Borophosphate Glasses. *Journal of Non-Crystalline Solids*, **355**, 229-234. https://doi.org/10.1016/j.jnoncrysol.2008.11.018

[21] Prashant Kumar, M. and Sankarappa, T. (2008) DC Conductivity in Some Alkali Doped Vanadotellurite Glasses. *Solid State Ionics*, **178**, 1719-1724. https://doi.org/10.1016/j.ssi.2007.11.003

[22] Devidas, G.B., Sankarappa, T., Chougule, B.K. and Prasad, G. (2007) DC Conductivity in Single and Mixed Alkali Vanadophosphate Glasses. *Journal of Non-Crystalline Solids*, **353**, 426-434. https://doi.org/10.1016/j.jnoncrysol.2006.12.011

[23] Greaves, G.N. and Ngai, K.L. (1995) Reconciling Ionic-Transport Properties with Atomic Structure in Oxide Glasses. *Physical Review B*, **52**, 6358-6380. https://doi.org/10.1103/PhysRevB.52.6358

[24] Rao, P.V., Raju, G.N., Prasad, P.S., Laxmikanth, C. and Veeraiah, N. (2016) Transport and Spectroscopic Properties of Nickel Ions in ZnO-B_2O_3-P_2O_5 Glass System. *Optik*, **127**, 2920-2923. https://doi.org/10.1016/j.ijleo.2015.12.056

[25] Nagaraja, N., Sangamesh, J., Chandrashekar, Sankarappa, T. and Ashwajeeth, J.S. (2016) Mixed Conduction in Alkali and Transition Metal Ion Doped Borate Glasses. 2016 *International Conference on Electrical, Electronics, and Optimization Techniques* (*ICEEOT*), Chennai, 3-5 March 2016, 1035-1039. https://doi.org/10.1109/ICEEOT.2016.7754843

[26] Nikolić, J., Pavić, L., Šantić, A., Mošner, P., Koudelka, L., Pajić, D. and Moguš-Milanković, A. (2018) Novel Insights into Electrical Transport Mechanism in Ionic-Polaronic Glasses. *Journal of the American Ceramic Society*, **101**, 1221-1235. https://doi.org/10.1111/jace.15271

[27] Isard, J.O. (1969) The Mixed Alkali Effect in Glass. *Journal of Non-Crystalline Solids*, **1**, 235-261. https://doi.org/10.1016/0022-3093(69)90003-9

[28] Vessal, B., Greaves, G.N., Marten, P.T., Chadwick, A.V., Mole, R. and Houde-Walter, S. (1992) Cation Microsegregation and Ionic Mobility in Mixed Alkali Glasses. *Nature*, **356**, 504-506. https://doi.org/10.1038/356504a0

[29] Hirashima, H., Nishii, K. and Yoshida, T. (1983) Electrical Conductivity of TiO_2-V_2O_5-P_20_5 Glasses. *Journal of the American Ceramic Society*, **66**, 704-708. https://doi.org/10.1111/j.1151-2916.1983.tb10533.x

[30] Malge, A., Sankarappa, T., Sujatha, T., Devidas, G.B. and Azeem, P.A. (2020) Investigation of Physical and Spectroscopic Properties of WO_3 Doped Zinc-Lithium-Dysprosium Borotellurite Glasses. *Optical Materials*, **109**, Article ID: 110282. https://doi.org/10.1016/j.optmat.2020.110282

[31] Cullity, B.D. (1956) Elements of X-Ray Diffraction. Addison-Wesley Publishing Company, Boston. http://117.239.25.194:7000/jspui/bitstream/123456789/954/1/PRELIMINARY%20AND%20CONTENT.pdf

[32] Rajashekara, G., Sangamesh, J., Arunkumar, B., Nagaraja, N., and Kumar, M.P. (2018) Anomalous DC Electrical Conductivity in Mixed Transition Metal Ions Doped Borate Glasses. *Journal of Non-Crystalline Solids*, **481**, 289-294. https://doi.org/10.1016/j.jnoncrysol.2017.10.056

[33] Greaves, G.N. (1973) Small Polaron Conduction in V_2O_5□P_2O_5 Glasses. *Journal of Non-Crystalline Solids*, **11**, 427-446. https://doi.org/10.1016/0022-3093(73)90089-6

[34] Dutta, B., Fahmy, N.A. and Pegg, I.L. (2006) Effect of Mixed Transition-Metal Ions in Glasses. Part III: The P_2O_5-V_2O_5-MnO System. *Journal of Non-Crystalline Solids*, **352**, 2100-2108. https://doi.org/10.1016/j.jnoncrysol.2006.02.043

[35] Mott, N.F. (1969) Conduction in Non-Crystalline Materials. *The Philosophical Magazine*: *A Journal of Theoretical Experimental and Applied Physics*, **19**, 835-852. https://doi.org/10.1080/14786436908216338

[36] Mott, N. and Davis, E. (2012) Electronic Processes in Non-Crystalline Materials. Oxford University Press, Oxford. https://books.google.com/books?hl=en&lr=&id=Pl1b_yhKH-YC&oi=fnd&pg=PP1&dq=N.+Mott+and+E.+Davis,+Electronic+processes+in+non-crystalline+materials.+2012&ots=d7xSbyBZXd&sig=3bXFSLTdenMPwXUMyB6OLIoVxxk

[37] Austin, I.G. and Mott, N.F. (1969) Polarons in Crystalline and Non-Crystalline Materials. *Advances in Physics*, **18**, 41-102. https://doi.org/10.1080/00018736900101267

[38] Salman, F.E. Shash, N., El-Haded, A.H. and El-Mansy, M.K. (2002) Electrical Conduction and Dielectric Properties of Vanadium Phosphate Glasses Doped with Lithium. *Journal of Physics and Chemistry of Solids*, **63**, 1957-1966. https://doi.org/10.1016/S0022-3697(02)00164-6

[39] El-Desoky, M.M. (2003) DC Conductivity and Hopping Mechanism in V_2O_5-B_2O_3-BaO Glasses. *Physica Status Solidi A*, **195**, 422-428. https://doi.org/10.1002/pssa.200305944

[40] Sujatha, T., Sankarappa, T., Ashwajeet, J.S., Ramanna, R. and Hanagodimath, S.M. (2015) Electrical Conduction in V_2O_5 Doped Borophosphate Glasses. *Journal of Advanced Chemical Sciences*, **1**, 157-159.

[41] Souri, D., Azizpour, P. and Zaliani, H. (2014) Electrical Conductivity of V_2O_5-TeO_2-Sb Glasses at Low Temperatures. *Journal of Electronic Materials*, **43**, 3672-3680. https://doi.org/10.1007/s11664-014-3288-x

[42] El-Desoky, M.M. (2005) Characterization and Transport Properties of V_2O_5-Fe_2O_3-TeO_2 Glasses. *Journal of Non-Crystalline Solids*, **351**, 3139-3146. https://doi.org/10.1016/j.jnoncrysol.2005.08.004

[43] Chakraborty, S., Sadhukhan, M., Modak, D.K. and Chaudhuri, B.K. (1995) Non-Adiabatic Polaron Hopping Conduction in Semiconducting V_2O_5-Bi_2O_3 Oxide Glasses Doped with $BaTiO_3$. *Journal of Materials Science*, **30**, 5139-5145. https://doi.org/10.1007/BF00356061

[44] Sakata, H., Sega, K. and Chaudhuri, B.K. (1999) Multiphonon Tunneling Conduction in Vanadium-Cobalt-Tellurite Glasses. *Physical Review B*, **60**, 3230-3236. https://doi.org/10.1103/PhysRevB.60.3230

[45] Emin, D. and Holstein, T. (1969) Studies of Small-Polaron Motion IV. Adiabatic Theory of the Hall Effect. *Annals of Physics*, **53**, 439-520. https://doi.org/10.1016/0003-4916(69)90034-7

[46] Ashwajeet, J.S., Sankarappa, T., Sujatha, T. and Ramanna, R. (2018) Thermal and Electrical Properties of (B_2O_3-TeO_2-Li_2O-CoO) Glasses. Journal of Non-Crystalline Solids, **486**, 52-57. https://doi.org/10.1016/j.jnoncrysol.2018.02.010

[47] Ghosh, A. and Chaudhuri, B.K. (1986) DC Conductivity of V_2O_5-Bi_2O_3 Glasses. *Journal of Non-Crystalline Solids*, **83**, 151-161. https://doi.org/10.1016/0022-3093(86)90065-7

[48] Abrahams, E., Anderson, P.W., Licciardello, D.C. and Ramakrishnan, T.V. (1979) Scaling Theory of Localization: Absence of Quantum Diffusion in Two Dimensions. *Physical Review Letters*, **42**, 673-676. https://doi.org/10.1103/PhysRevLett.42.673

[49] Anderson, P.W. (1958) Absence of Diffusion in Certain Random Lattices. *Physical Review*, **109**, 1492-1505. https://doi.org/10.1103/PhysRev.109.1492

[50] Al-Assiri, M.S., Salem, S.A. and El-Desoky, M.M. (2006) Effect of Iron Doping on the Characterization and Transport Properties of Calcium Phosphate Glassy Semiconductors. *Journal of Physics and Chemistry of Solids*, **67**, 1873-1881. https://doi.org/10.1016/j.jpcs.2006.04.015